Inorganic Chemistry

Article

pubs.acs.org/IC

Investigating the Complexation of the Pb^{2+}/Bi^{3+} Pair with Dipicolinate Cyclen Ligands

Luís M. P. Lima,[†,‡] Maryline Beyler,[†] Rita Delgado,*[,‡] Carlos Platas-Iglesias,*[,§] and Raphaël Tripier*[,†]

[†]Université de Bretagne Occidentale, UMR-CNRS 6521, UFR des Sciences et Techniques, 6 avenue Victor le Gorgeu, C.S. 93837, 29238 BREST Cedex 3, France

[‡]Instituto de Tecnologia Química e Biológica António Xavier, Universidade Nova de Lisboa, Av. da República, 2780-157 Oeiras, Portugal

[§]Departamento de Química Fundamental, Facultade de Ciencias, Universidade da Coruña, Campus da Zapateira-Rúa da Fraga 10, 15008 A Coruña, Spain

Supporting Information

ABSTRACT: The complexation properties toward Pb^{2+} and Bi^{3+} of the macrocyclic ligands 6,6′-((1,4,7,10-tetraazacyclododecane-1,7-diyl)bis(methylene))dipicolinic acid (H_2**do2pa**) and 6,6′-((4,10-dimethyl-1,4,7,10-tetraazacyclododecane-1,7-diyl)bis(methylene))dipicolinic acid (H_2**Me-do2pa**) have been investigated. A new three-step synthesis of H_2**do2pa** following the bisaminal methodology has also been developed. The X-ray structures of [Pb(**Me-do2pa**)]·$6H_2O$ and [Bi(**Me-do2pa**)](NO_3)·H_2O show that the two metal ions are eight-coordinated by the ligand. The two complexes exist as the racemic $\Delta(\delta\delta\delta\delta)/\Lambda(\lambda\lambda\lambda\lambda)$ mixture both in the solid state and in solution, as indicated by NMR and DFT studies. The stability constants of the lead(II) and bismuth(III) complexes of the two ligands were determined in 0.5 M KCl using potentiometric and spectrophotometric techniques. The stability constants determined for the complexes of Pb^{2+} are relatively high (log K_{ML} = 16.44 and 18.44 for H_2**do2pa** and H_2**Me-do2pa**, respectively) and exceptionally high for the complexes of Bi^{3+} (log K_{ML} = 32.0 and 34.2 for H_2**do2pa** and H_2**Me-do2pa**, respectively). The [Pb(**Me-do2pa**)] complex presents rather fast formation and very good kinetic inertness toward transchelation. Additionally, the [Bi(**Me-do2pa**)]$^+$ complex was found to present a remarkably fast complexation rate (full complexation in ∼2 min at pH 5.0, acetate buffer) and a very good kinetic inertness with respect to metal ion dissociation (half-life of 23.9 min in 1 M HCl), showing promise for potential applications in α-radioimmunotherapy.

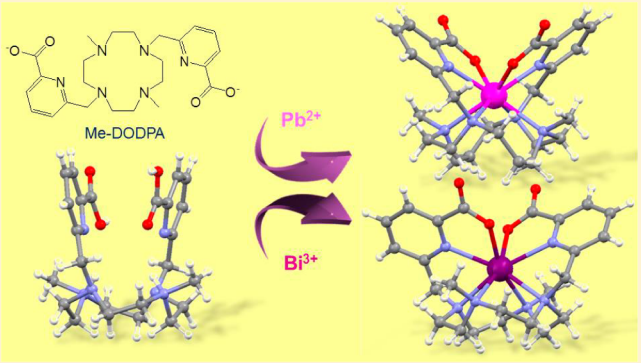

INTRODUCTION

There is a growing interest in the coordination chemistry of Pb^{2+} and Bi^{3+} ions due to the potential application of their ^{212}Pb, ^{212}Bi, and ^{213}Bi radioisotopes as potential therapeutic agents.[1] In fact, ^{212}Bi (half-life = 61 min) and ^{213}Bi (half-life = 46 min) are among the few α-particle emitting radionuclides that have properties suitable for developing therapeutic agents.[2,3] However, the short half-life of these radionuclides limits their application to tumor cells that can be accessed rapidly by the targeting agent. To circumvent this problem, the β^--emitter ^{212}Pb (half-life = 10.2 h) can be used as an *in situ* generator of ^{212}Bi, thereby effectively extending the half-life of radioactive bismuth to about 11 h.[4,5] This strategy also allows avoiding the direct complexation of Bi^{3+} that usually is perturbed by the formation of hydroxides even at acidic pH[6] and constitutes an important drawback for its application as radiopharmaceutical. The long path length of β^- radiation makes β^--emitting radionuclides best suited for application to relatively large solid tumors, while the shorter path length of α-particles makes ^{212}Bi and ^{213}Bi useful for the treatment of patients with micrometastases or hematological cancer.[7]

The design of ligands for $^{212}Pb/^{212}Bi$ *in situ* generators is a challenging task for coordination chemists, as it requires chelators not only with a high affinity for both Pb^{2+} and Bi^{3+} in terms of thermodynamic stability and kinetic inertness but also with fast complexation kinetics with the former cation.[8] A high thermodynamic stability and kinetic inertness are crucial to avoid the release of toxic metal ions *in vivo*. Indeed, it is well-known that Pb^{2+} is very toxic,[9] as it accumulates in soft tissues including vital organs such as the brain originating severe neurological and/or hematological effects.[10] On the other hand, bismuth compounds present relatively low toxicity as compared to related species containing heavy metals, and actually bismuth compounds remain important components of a number of remedies used for the treatment of gastrointestinal problems;

Received: May 13, 2015
Published: July 6, 2015

DOI: 10.1021/acs.inorgchem.5b01079
Inorg. Chem. 2015, 54, 7045−7057

Chart 1

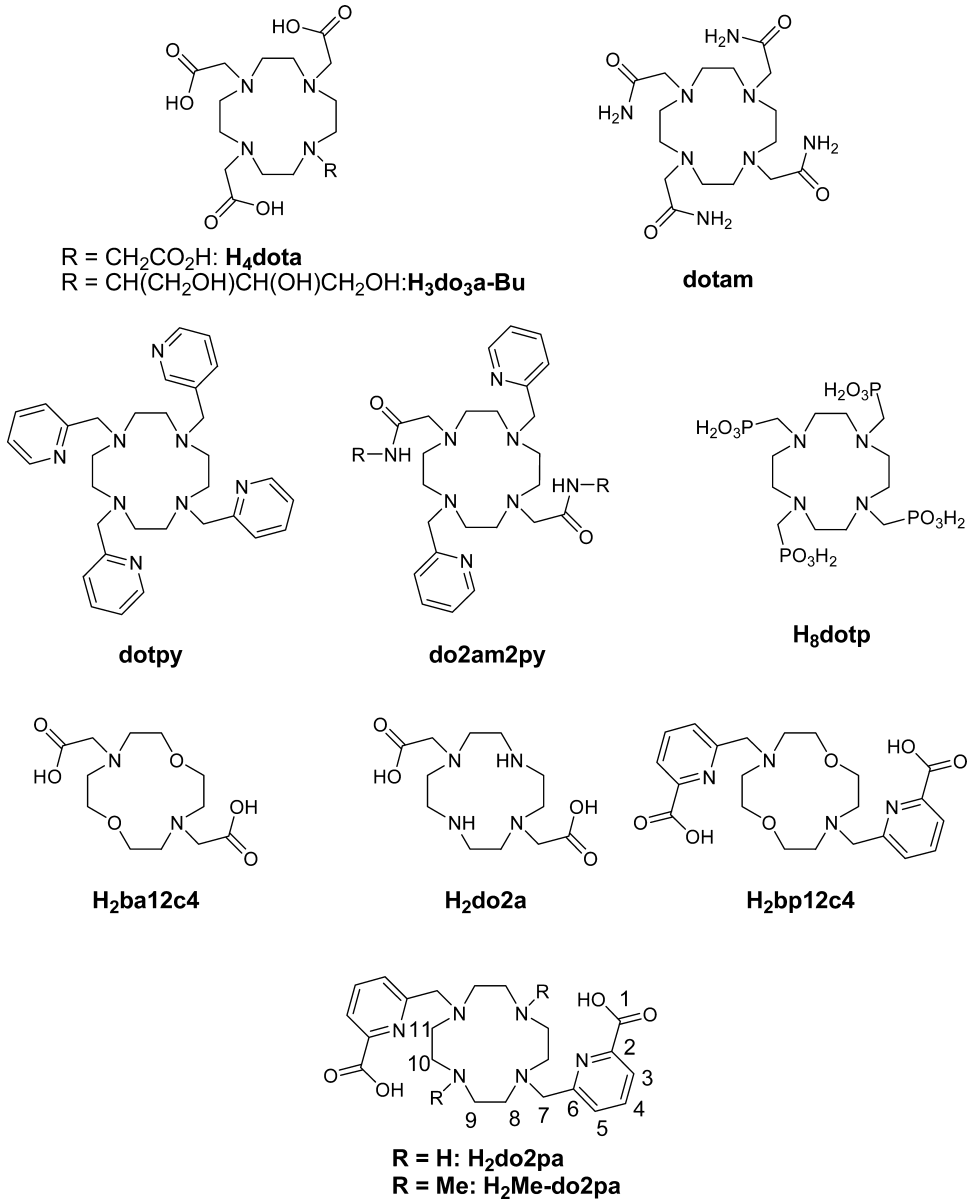

for instance, bismuth(III) citrate has been successfully used to treat ulcers.[11]

Both Pb^{2+} and Bi^{3+} exhibit a high affinity for ligands containing either N or N and O donor atoms,[12] and often adopt high coordination numbers (6−10) and irregular coordination geometries imposed by the nature of the multidentate ligand system. Tetraazacycloalkane derivatives are often the ligands of choice for lead(II) complexation, particularly cyclen-based ligands. The macrocyclic framework is able to accept four additional chelating groups by functionalization of the cyclic amines. The outstanding properties of the tetraacetamide derivative of cyclen (dotam, see Chart 1) for lead(II) coordination were first reported in 1995 by Maumela et al.[13] The physicochemical properties and structural studies of the $[Pb(dotam)]^{2+}$ complex were noteworthy completed by Hancock and colleagues in 2004[14] and then Guilard and colleagues in 2008.[15] The $[Pb(dota)]^{2-}$ complex was also reported to be very stable in aqueous solution.[16] Tetraazacycloalkane-based ligands have also been used for bismuth(III) coordination. For instance, the stability and solution structure and dynamics of the bismuth(III) complexes of H_4dota and its butriol derivative H_3do3a-Bu have been reported.[17] The octadentate ligand H_8dotp was also found to provide fast complexation of both Pb(II) and Bi(III), with the resulting complexes being very stable.[18] The DNA-binding properties and the antitumor activity of the bismuth(III) complex of 1,4,7,10-tetrakis(2-pyridylmethyl)-1,4,7,10-tetraazacyclododecane (dotpy, Chart 1) were also reported.[19] These studies demonstrated that the complex of Bi^{3+} is able to induce conformational changes of DNA under physiological conditions. More recently, we fully studied and characterized the structure of the $[Bi(dotpy)]^{3+}$ complex as well as that of its very close derivative, do2am2py, bearing two pyridylmethyl and two acetamide arms.[20] These studies demonstrated that aromatic 2-pyridylmethyl substituents are good chelating functions for Bi^{3+}.

To our knowledge, cyclen-based ligands bearing picolinate pendant arms have never been used for complexation of Pb^{2+},

DOI: 10.1021/acs.inorgchem.5b01079
Inorg. Chem. 2015, 54, 7045−7057

Scheme 1. Synthetic Route for H_2do2pa

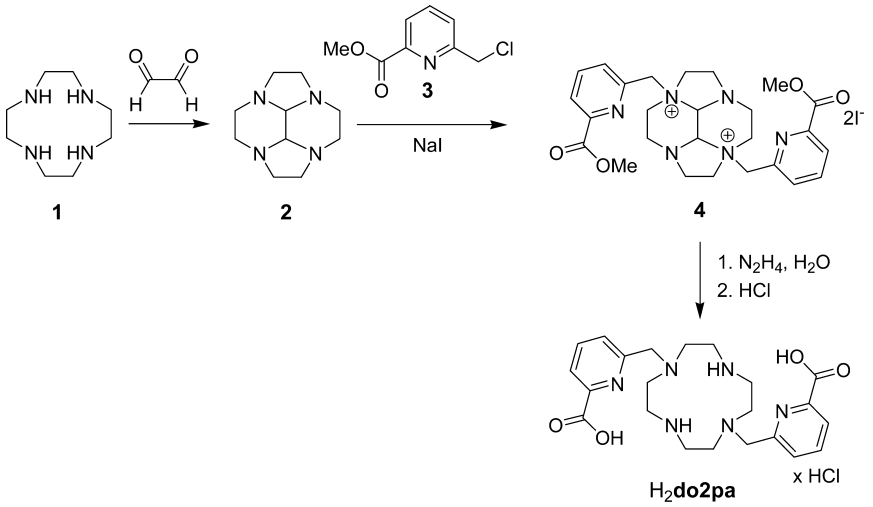

and only very recently, the complexation of Bi^{3+} has been the subject of a brief communication.[21] Chelates containing picolinate groups such as H_2**do2pa** and H_2**Me-do2pa** (Chart 1) should offer a N_6O_2 donor set to the metal center. A very close analogue, H_2bp12c4, was proven to be quite a good ligand for lead(II).[22] Following recent studies that showed that H_2**do2pa** and H_2**Me-do2pa** are strong chelators for the lanthanide ions,[23,24] we found these ligands also attractive for the sequestration of Pb^{2+} and Bi^{3+} cations, which as the lanthanides often prefer high coordination numbers. Picolinate arms have the obvious advantage of providing two donor atoms in the same group, which renders two secondary amines of the macrocyclic skeleton available to prepare bifunctional chelating agents (BCAs) via their functionalization, besides allowing for derivatization of the carboxylic acid group of the picolinate as well.

In a recent communication, we disclosed a preliminary characterization of the [Bi(**Me-do2pa**)]$^+$ complex both in the solid state and in solution, as well as ^{213}Bi labeling studies.[21] Herein we report a full study of the coordination properties of the cyclen-based ligands H_2**do2pa** and H_2**Me-do2pa** toward Pb^{2+} and Bi^{3+}, with the aim of validating these ligands as potential chelators for the development of ^{212}Pb/^{212}Bi *in situ* generators. A new synthesis of the H_2**do2pa** ligand is also presented. The acid−base properties of the two ligands and the stability constants of their complexes with Pb^{2+} and Bi^{3+} were determined. The complexes of both chelators were synthesized and characterized using X-ray diffraction, UV−vis, and NMR spectroscopies and density functional theory (DFT) calculations. The formation kinetics of the complexes and their inertness toward proton-assisted dissociation was also studied.

RESULTS AND DISCUSSION

Synthesis of the Ligands and Their Lead(II) and Bismuth(III) Complexes. In a previous contribution,[23] we reported the synthesis of H_2**Me-do2pa** using bisaminal chemistry,[25] and that of H_2**do2pa** by following *trans*-alkylation of 1,7-diBoc-cyclen.[26] Herein we report an alternative synthesis of H_2**do2pa** using bisaminal chemistry (Scheme 1). Indeed, the synthesis of compound H_2**do2pa** was achieved by *trans*-alkylation of cyclen glyoxal **2**[27] with 6-chloromethylpyridine-2-carboxylic acid methyl ester **3**,[28] which resulted in the formation of the bisammonium salt **4** in 93% yield. Single crystals of the bishydrate of **4** (Figure 1) confirmed that alkylation of cyclen glyoxal takes place on two nitrogen atoms

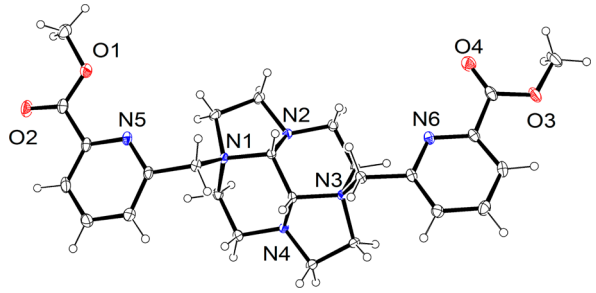

Figure 1. View of the crystal structure of the bisammonium salt **4**. Water molecules and iodide anions were removed for simplicity. The ORTEP plot is at the 30% probability level.

in the *trans* position that have their lone pairs pointing to the convex side of the molecule.[27] The reductive cleavage of **4** with hydrazine monohydrate resulted in the quantitative formation of an intermediate bis-acetohydrazide derivative, which was directly submitted to hydrolysis to give the desired ligand with an overall yield of 61% as calculated from cyclen.

Slow evaporation of a water solution containing the H_2**Me-do2pa** ligand as a hydrochloride salt gave single crystals suitable for X-ray diffraction. Crystallographic data are not good enough to be fully discussed here (see Figure S1 and Table S1 in the Supporting Information), but nevertheless, the X-ray crystal structure of the [H_4**Me-do2pa**]$^{2+}$ cation is very similar to that of the trifluoroacetate salt reported previously.[24] Indeed, two *trans* N atoms of the cyclen unit containing methyl substituents are protonated, while the 12-membered macrocycle adopts a square [3333] conformation similar to that observed for protonated forms of dota^{4-} and related ligands, in which the ligand is predisposed to bind metal ions.

The complexes of Bi^{3+} and of Pb^{2+} (Scheme 2) were synthesized by addition of 1 equiv of the metal ion to an aqueous solution of the ligand hydrochloride followed by adjustment of the pH to 3−4 (Bi^{3+}) or 6−7 (Pb^{2+}). The resulting complexes were separated from inorganic salts by successive precipitation from methanol and isolated in good yields for the bismuth(III) complexes (60−80%) and almost

DOI: 10.1021/acs.inorgchem.5b01079
Inorg. Chem. 2015, 54, 7045−7057

Scheme 2. Synthesis of the Bismuth(III) and Lead(II) Complexes

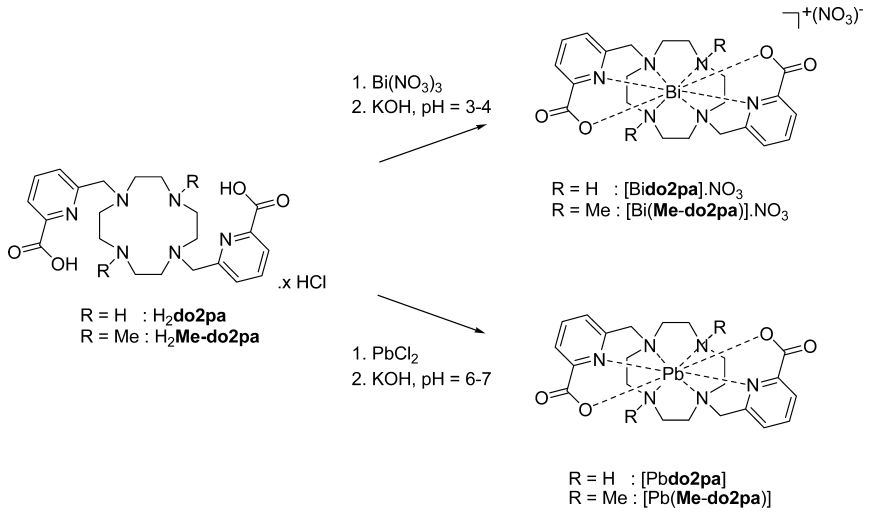

quantitatively for the lead(II) complexes. All complexes were then characterized in solution by ^{1}H and ^{13}C NMR and HRMS.

X-ray Crystal Structures of [Pb(Me-do2pa)]·6H$_2$O and [Bi(Me-do2pa)](NO$_3$)·H$_2$O. Single crystals of the lead(II) and bismuth(III) complexes with **Me-do2pa**$^{2-}$ were obtained by slow evaporation of aqueous solutions of the isolated complexes. The X-ray of the bismuth(III) complex was presented in a previous communication,[21] and it is described here for comparative purposes. Crystals of the lead(II) complex contain the [Pb(**Me-do2pa**)] entity and disordered water molecules. Figure 2 shows views of the structures of both the Pb^{2+} and Bi^{3+} complexes, while bond distances of the metal coordination environments are given in Table 1.

The metal ions are directly bound to the eight donor atoms of the ligand, which presents a *syn* conformation with the two pendant arms disposed on the same side of the macrocyclic unit. The two complexes present a crystallographically imposed C_2 symmetry, where the symmetry axis is perpendicular to the plane defined by the four nitrogen atoms of the macrocycle and contains the metal ion. The distances between the Bi center and the nitrogen atoms of the cyclen unit are ca. 0.12 Å longer than the Bi(1)−N(3) distances. However, in the case of the lead(II) complex, the Pb−N distances fall in a narrower range (ca. 2.68−2.73 Å, Table 1). Furthermore, the Pb(1)−O(1) distance of 2.692(3) Å is very similar to the Pb−N distances, while for the bismuth(III) complex the Bi(1)−O(1) distance of 2.390(3) Å is considerably shorter than the Bi−N distances (2.50−2.63 Å). These data probably reflect the harder nature as a Lewis acid of Bi^{3+} compared to Pb^{2+} according to the Pearson HSAB classification,[29] which results in a more important tendency of Bi^{3+} to bind to the (harder) oxygen donor atoms of the ligand, and a preference of Pb^{2+} to interact with the (softer) nitrogen donor atoms. The hard nature of the metal ion is more evident in the case of the Eu^{3+} and Lu^{3+} complexes reported previously, for which the bond distances involving the oxygen atoms of the ligand are even shorter when compared to the distances to nitrogen atoms.[30] The distances between Bi and the donor atoms of the cyclen unit are ca. 0.1 Å longer than the average Bi−N distance observed for [Bi(dota)]$^-$ (2.53 Å).[17]

The Pb−O distance of 2.692(3) Å in [Pb(**Me-do2pa**)] is considerably shorter than the average Pb−O distance reported recently for the [Pb(dota)]$^{2-}$ complex (2.77 Å), which presents three relatively long Pb−O distances (ca. 2.80−2.86 Å) and a

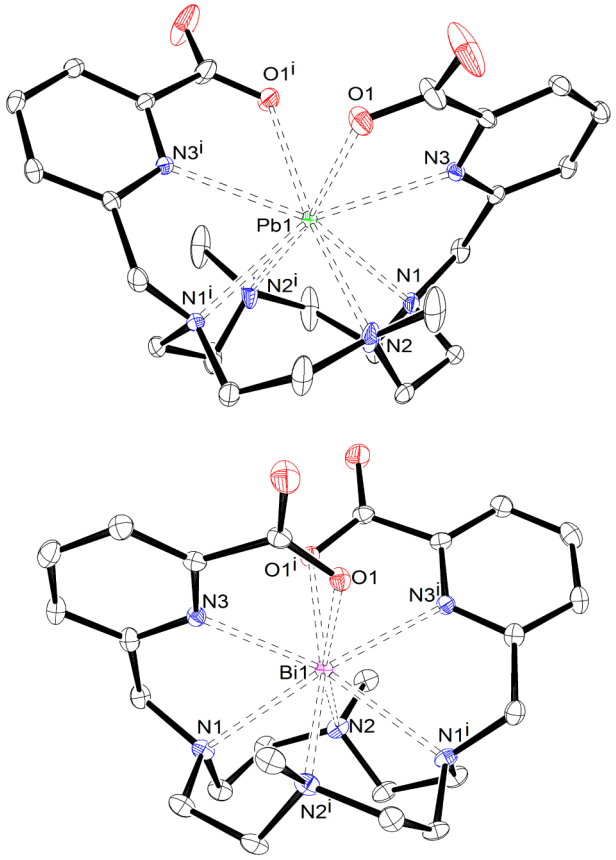

Figure 2. X-ray crystal structures of [Pb(**Me-do2pa**)] (top) and [Bi(**Me-do2pa**)]$^+$ (bottom) complexes with atom labeling; hydrogen atoms and anions are omitted for simplicity. The ORTEP plots are drawn at the 30% probability level.

relatively short one (2.61 Å).[31] Furthermore, the Pb−N distances determined for [Pb(dota)]$^{2-}$ (average at 2.66 Å) are somewhat shorter than the Pb−N1 and Pb−N2 distances in [Pb(**Me-do2pa**)]. These data support the structure of [Pb(**Me-do2pa**)] is holodirected, with the Pb^{2+} lone pair being stereochemically inactive, as often observed for complexes with high coordination numbers.[32,33] On the contrary, the lone pair of Pb^{2+} appears to be active in [Pb(dota)]$^{2-}$, resulting in a

DOI: 10.1021/acs.inorgchem.5b01079
Inorg. Chem. 2015, 54, 7045−7057

Table 1. Selected Bond Lengths (Å) and Angles (deg) of the Metal Coordination Environment in [Pb(Me-do2pa)] and [Bi(Me-do2pa)]$^+$ Complexes and Related Complexes Reported in the Literature[a]

	Pb	Bi	Eu[b]	Lu[b]
M(1)−O(1)	2.692(3)	2.390(3)	2.325(2)	2.236(2)
M(1)−N(1)	2.727(3)	2.633(4)	2.595(2)	2.517(3)
M(1)−N(2)	2.701(4)	2.620(4)	2.593(2)	2.522(2)
M(1)−N(3)	2.678(3)	2.503(4)	2.471(2)	2.380(2)

[a]See Figure 2 for labeling. [b]Data taken from ref 30.

hemidirected structure with long Pb−O bonds. We also notice that the Bi−O distances in [Bi(dota)]$^-$ are longer than the Bi−N bonds, in contrast to the situation observed for [Bi(**Me-do2pa**)]$^+$, which suggests a certain degree of stereochemical activity of the Bi^{3+} lone pair in the former.

As described in detail for different complexes of cyclen-based ligands,[34] the *syn* conformation of the ligand in the **Me-do2pa**$^{2-}$ complex implies the occurrence of two helicities (one belonging to the cyclen moiety and one associated with the layout of the pendant arms). Inspection of the crystal structure data reveals that in both the lead(II) and bismuth(III) complexes two $\Delta(\delta\delta\delta\delta)$ and $\Lambda(\lambda\lambda\lambda\lambda)$ enantiomers cocrystallize in equal amounts.[35,36] The coordination polyhedron can be described as a distorted twisted-square antiprism (TSAP) comprised of two parallel pseudo planes: the donor atoms of the pendant arms define the upper pseudo plane, while the nitrogen atoms of the cyclen unit define the lower plane. However, the upper plane presents very important deviations from planarity, which amount to 0.51 and 0.38 Å for the lead(II) and bismuth(III) complexes, respectively. The mean twist angles, ω,[37] between these nearly parallel squares are −16.4° (Pb) and −21.2° (Bi), in line with a more important distortion of the TSAP geometry toward a cube in the case of the lead(II) complex.

Structure of the Complexes of H_2Me-do2pa in Solution. The ^{1}H and ^{13}C NMR spectra of the bismuth(III) complex of H_2**Me-do2pa** were reported in a preliminary communication.[21] The spectra pointed to a very rigid structure of the complex that indicates the presence of a single diastereoisomer in solution with an effective C_2 symmetry. In contrast, the ^{1}H and ^{13}C NMR spectra recorded in D_2O solution for [Pb(**Me-do2pa**)] point to a fluxional behavior due to intramolecular exchange processes (Figure 3). Indeed, the ^{1}H NMR spectrum of [Pb(**Me-do2pa**)] recorded at pD 8.2 and 278 K shows relatively broad signals for the proton nuclei of the cyclen unit. These proton signals become even broader upon increasing temperature, achieving coalescence in the temperature range 298−308 K. The spectra recorded at high temperatures are consistent with an effective C_{2v} symmetry in solution. Unfortunately, the slow exchange region is not achieved at the lowest temperature investigated (278 K), which prevented a full line-shape analysis to determine the activation parameters for the exchange process. However, the signals due to protons H7 could be clearly identified in the spectrum recorded at 278 K (4.65 and 4.10 ppm), which points to a C_2 symmetry of the complex in solution. These signals achieve coalescence at a temperature of ca. 300 K, which allows us to estimate an activation free energy for the dynamic process of $\Delta G^{\ddagger}$ = 58 kJ mol^{-1}. This activation free energy is very similar to those determined for [Pb(dotam)]$^{2+}$ using ^{13}C NMR spectroscopy (62−64 kJ mol^{-1}).[13,15]

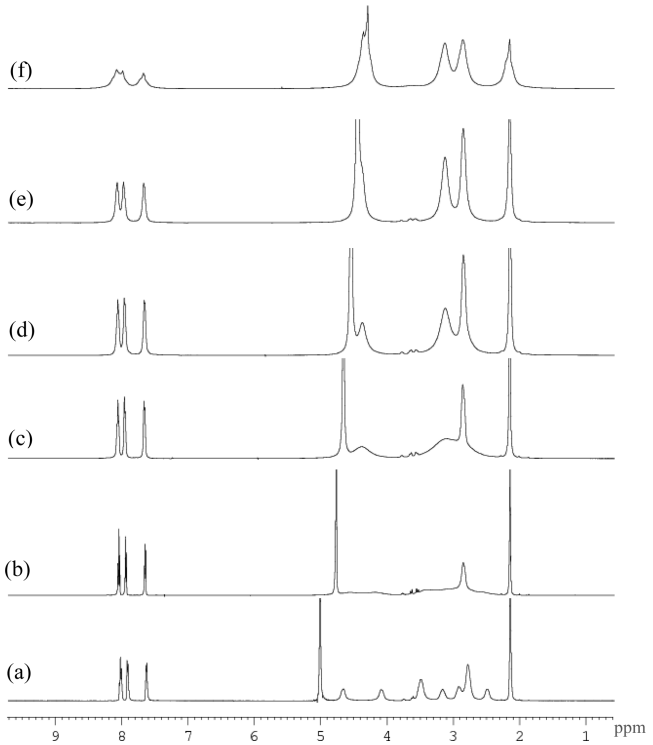

Figure 3. ^{1}H NMR (pD 8.2, 500 MHz) of the [Pb(**Me-do2pa**)] complex at (a) 278 K, (b) 298 K, (c) 308 K, (d) 318 K, (e) 328 K, and (f) 343 K.

To gain insight into the solution structure and dynamics of the [Pb(**Me-do2pa**)] complex, we carried out DFT calculations in aqueous solution (see computational details below). As described previously for the complexes of bp12c4^{2-},[22] there are four possible diastereoisomeric forms of the [Pb(**Me-do2pa**)] complex compatible with a C_2 symmetry: $\Delta(\delta\delta\delta\delta)$, $\Delta(\lambda\lambda\lambda\lambda)$, $\Delta(\delta\lambda\delta\lambda)$, and $\Delta(\lambda\delta\lambda\delta)$. Geometry optimizations carried out at the TPSSh/ECP60MDF/6-31G(d) level provide four energy minima corresponding to these diastereoisomeric forms. According to our calculations, the minimum energy conformation corresponds to the $\Delta(\delta\delta\delta\delta)$ isomer, with the relative free energies of the $\Delta(\lambda\lambda\lambda\lambda)$, $\Delta(\delta\lambda\delta\lambda)$, and $\Delta(\lambda\delta\lambda\delta)$ isomers being 11.30, 19.96, and 51.34 kJ mol^{-1}, respectively. Thus, our calculations indicate that the [Pb(**Me-do2pa**)] complex exists in aqueous solution as the $\Delta(\delta\delta\delta\delta)/\Lambda(\lambda\lambda\lambda\lambda)$ enantiomeric pair, in line with the structure observed in the solid state. Therefore, the dynamic process observed by NMR spectroscopy for [Pb(**Me-do2pa**)] is likely related to a $\Delta(\delta\delta\delta\delta) \leftrightarrows \Lambda(\lambda\lambda\lambda\lambda)$ interconversion, which requires both the inversion of the macrocyclic unit and the rotation of the picolinate pendant arms.

The ring inversion process of [Pb(**Me-do2pa**)] was investigated using DFT calculations following the methodology reported in earlier studies.[38] According to our calculations, the inversion of the macrocyclic unit is a four-step process, each of them involving a $\delta \leftrightarrows \lambda$ conformational change of a five-membered chelate ring formed due to the coordination of the macrocyclic unit to the Pb^{2+} ion (Figure 4). The free energy barrier for the ring inversion process was estimated from the energy of the transition state with the highest energy (TS4, Figure 3), which resulted in being 62.5 kJ mol^{-1}. This value is very similar to that determined experimentally from NMR measurements (58 kJ mol^{-1}), suggesting that either the ring

DOI: 10.1021/acs.inorgchem.5b01079
Inorg. Chem. 2015, 54, 7045−7057

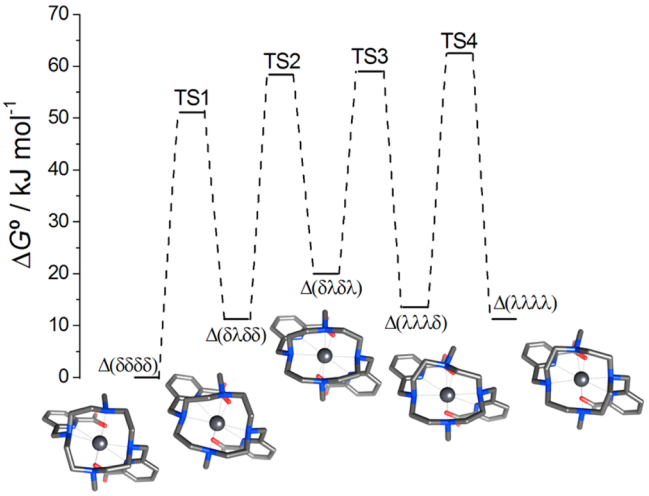

Figure 4. Relative free energies of energy minima and transition states involved in the ring inversion process of [Pb(**Me-do2pa**)].

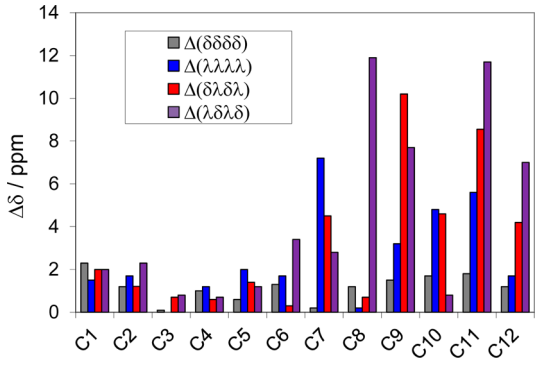

Figure 5. Absolute differences between experimental and theoretical ^{13}C NMR shifts (TPSSh/ECP60MDF/EPR-III level) for the different conformations of [Bi(**Me-do2pa**)]$^{+}$. See Chart 1 for labeling.

inversion is the rate-determining step for the $\Delta(\delta\delta\delta\delta) \leftrightarrows \Lambda(\lambda\lambda\lambda\lambda)$ interconversion or both the ring-inversion and arm rotation processes proceed with comparable rates. The activation energy calculated for the ring inversion process is very similar to those determined experimentally and computationally for lead(II),[13,15] bismuth(III),[17] and lanthanide(III)[39] complexes with cyclen-based ligands, which typically fall within the range 56−65 kJ mol^{-1}. These results suggest that the energy barriers of the cyclen inversion processes in this class of complexes do not vary significantly depending on the nature of the metal ion.

In order to confirm that [Bi(**Me-do2pa**)]$^{+}$ adopts the $\Delta(\delta\delta\delta\delta)$ structure in solution suggested by the X-ray crystal structure, we have also performed DFT calculations at the TPSSh/ECP60MDF/6-31G(d) level. The calculated relative free energies predict that the $\Delta(\delta\delta\delta\delta)$ isomer corresponds to a global minimum, with the relative free energies of the $\Delta(\lambda\lambda\lambda\lambda)$, $\Delta(\delta\lambda\delta\lambda)$, and $\Delta(\lambda\delta\lambda\delta)$ isomers being 9.00, 21.91, and 62.19 kJ mol^{-1}, respectively. To confirm the predictions made on the basis of the relative energies, we have calculated the ^{13}C NMR chemical shifts of the four isomers at the TPSSh/ECP60MDF/EPR-III level (Table S2 in the Supporting Information). It has been shown that the magnetic shieldings calculated with the use of ECPs are not gauge invariant, which means that magnetic shieldings calculated with different origins are different. However, the errors introduced by the violation of gauge invariance have been shown to be in the order of a few ppm, and therefore, ^{13}C NMR shifts can be calculated by this method with reasonably good accuracy.[40,41] Figure 5 shows the absolute deviations of the calculated NMR shifts from the experimental values ($\Delta\delta$) for the different isomers. The ^{13}C NMR shifts calculated for the $\Delta(\delta\delta\delta\delta)$ isomer are in very good agreement with the experimental data, with absolute deviations <2.3 ppm, while much larger deviations between the experimental and calculated data are obtained for the other isomers (up to ∼12 ppm, Figure 5). Thus, our calculations confirm that the [Bi(**Me-dodpa**)]$^{+}$ complex exists in solution as the $\Delta(\delta\delta\delta\delta)$/$\Lambda(\delta\delta\delta\delta)$ enantiomeric pair.

Protonation Constants of the Ligands and Stability Constants of Their Lead(II) and Bismuth(III) Complexes. The protonation constants of **do2pa**$^{2-}$ and **Me-do2pa**$^{2-}$ as well as the stability constants of their complexes with Pb^{2+} and Bi^{3+} were determined at 25 °C in 0.50 M KCl aqueous solution. The stepwise constants (log K) obtained are given in Table 2 together with protonation and stability constants reported for the related ligands bp12c4^{2-}, dota^{4-}, ba12c4^{2-}, and do2a^{2-} (Chart 1). The global constants (log β) and the corresponding standard deviations are collected in Table S3 in the Supporting Information. The protonation and Bi^{3+} complexation constants of **Me-do2pa**$^{2-}$ were reported in a preliminary communication.[21] The background electrolyte (KCl) and ionic strength (0.50 M) used for all equilibrium determinations were chosen because some of the determinations were done at very high pH (see below).

The protonation constants of **do2pa**$^{2-}$ and **Me-do2pa**$^{2-}$ determined by potentiometric titrations are overall fairly similar between the two ligands, although the first protonation constant of **Me-do2pa**$^{2-}$ is 0.6 log units higher than that of **do2pa**$^{2-}$ while the second protonation constant of **do2pa**$^{2-}$ is one log unit higher than that of **Me-do2pa**$^{2-}$. The first and second protonation processes occur at two opposite amines of the cyclen unit as usual for related systems such as dota^{4-},[42] possibly at the amines not bound to picolinate groups, as found on the X-ray structure of [H_4**Me-do2pa**]$^{2+}$.[24] The third and fourth protonation processes in **do2pa**$^{2-}$ and **Me-do2pa**$^{2-}$ are assigned to the carboxylate functions of the picolinate groups.[24,43] Both **do2pa**$^{2-}$ and **Me-do2pa**$^{2-}$ have protonation constants for the first and second protonation steps that are similar to do2a^{2-}. Thus, the decreased basicity often observed when carboxylate groups are replaced by picolinate moieties,[44] which is obvious when comparing the protonation constants determined for bp12c4^{2-} and ba12c4^{2-}, is not observed for the cyclen-based ligands reported here. However, the first protonation constant in **do2pa**$^{2-}$ is clearly lower than that determined for dota^{4-}, which can be attributed to the higher negative charge and higher ability to form strong hydrogen bonds of the latter ligand. The protonation constants obtained for both **do2pa**$^{2-}$ and **Me-do2pa**$^{2-}$ are in agreement with those reported in different experimental conditions.[24] Species distribution diagrams for both **do2pa**$^{2-}$ and **Me-do2pa**$^{2-}$ are shown at Figure S2 in the Supporting Information.

Potentiometric titrations of H_2**do2pa** and H_2**Me-do2pa** were carried out in the presence of Pb^{2+} to determine the stability constants of the corresponding metal complexes. Equilibrium was reached quickly enough during these in-cell titrations despite the relatively slow complex formation at acidic pH (see kinetic studies below). The speciation model is quite simple and similar in both H_2**do2pa** and H_2**Me-do2pa** systems,

DOI: 10.1021/acs.inorgchem.5b01079
Inorg. Chem. 2015, 54, 7045−7057

Table 2. Stepwise Protonation Constants (log K_{H_hL}) of do2pa^{2-} and Me-do2pa^{2-} and Stepwise Stability Constants (log K_{MH_hL}) of Their Complexes with Pb^{2+} and Bi^{3+} Metal Ions, at 25.0 °C and I = 0.50 M in KCl[a]

equilibrium reaction[b]	**do2pa^{2-}**	**Me-do2pa^{2-}**	bp12c4^{2-} [c]	dota^{4-}	ba12c4^{2-} [d]	do2a^{2-}
L + H^+ ⇄ HL	10.85(2)	11.45(3)	8.67	12.09;[e] 12.6[f]	9.53	10.91;[g] 11.45[h]
HL + H^+ ⇄ H_2L	9.92(3)	8.95(3)	6.90	9.76;[e] 9.70[f]	7.46	9.45;[g] 9.54[h]
H_2L + H^+ ⇄ H_3L	4.11(3)	4.17(3)	3.42	4.56;[e] 4.50[f]	2.11	4.09;[g] 4.00[h]
H_3L + H^+ ⇄ H_4L	2.91(2)	3.06(2)	1.67	4.09;[e] 4.14[f]		3.18;[g] 2.36[h]
H_4L + H^+ ⇄ H_5L				2.32[f]		
Pb^{2+} + L ⇄ PbL	16.44(2)	18.44(2)	15.44	22.69;[e] 24.3[i]	12.43	18.3[h]
PbL + H^+ ⇄ PbHL	3.63(7)	3.27(4)	2.52	3.86[e]		3.6[h]
PbLOH + H^+ ⇄ PbL	11.71(4)	11.29(4)				
Bi^{3+} + L ⇄ BiL	32.0(1)	34.2(1)		30.3[j]		
BiL + H^+ ⇄ BiHL		2.0(1)				
BiLOH + H^+ ⇄ BiL	11.8(1)	12.0(1)				

[a]Literature data for related systems are provided for comparison. [b]L denotes the ligand in general; charges of ligand and complex species were omitted for simplicity. [c]I = 0.1 M KNO_3, ref 22. [d]I = 0.1 M KNO_3, ref 45. [e]I = 0.1 M NMe_4Cl, ref 46. [f]I = 0.1 M NMe_4NO_3, ref 47. [g]I = 0.1 M KCl, ref 48. [h]I = 0.1 M NEt_4ClO_4, ref 49. [i]I = 0.1 M $NaClO_4$, ref 16. [j]I = 1.0 M NaBr, ref 17.

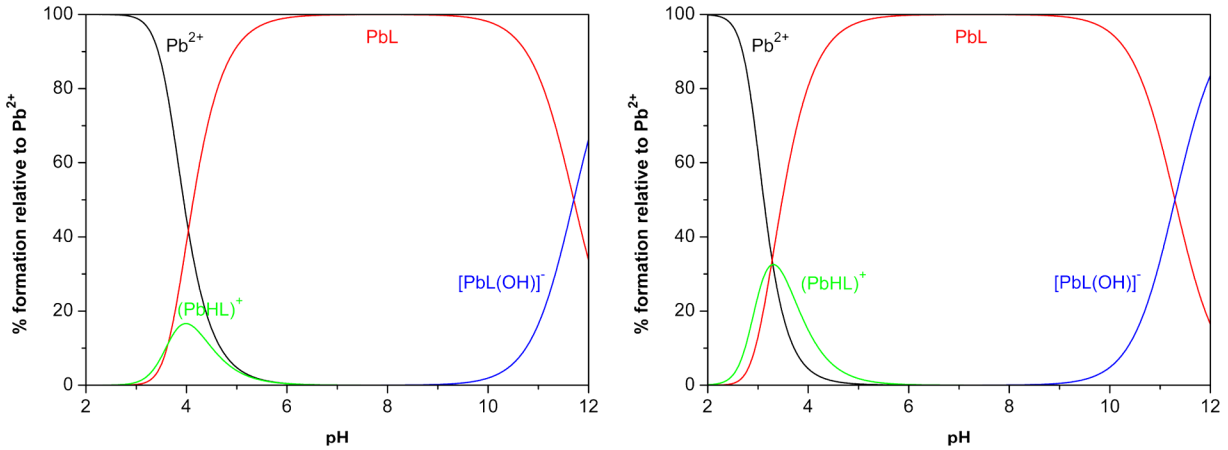

Figure 6. Species distribution diagrams of aqueous solutions of H_2**do2pa** (left) and H_2**Me-do2pa** (right) in the presence of Pb^{2+} at $[Pb^{2+}]_{tot} = [L]_{tot}$ = 1.0 mM.

containing only the PbLH, PbL, and PbL(OH) complex species. The stability constants given in Table 2 show that the complex of Pb^{2+} with H_2**Me-do2pa** is 2 log units more stable than with the H_2**do2pa** analogue despite the rather similar basicity of the two ligands. However, the lead(II) complex of H_4dota remains stronger, with a stability constant higher than that for [Pb(**Me-do2pa**)]. Interestingly, the stability constant of [Pb(**Me-do2pa**)] is three log units higher than that of [Pb(bp12c4)] but similar to that of [Pb(do2a)], which reflects the higher basicity of H_2**Me-do2pa** and H_2do2a when compared to H_2bp12c4 (Table 2). The species distribution diagrams calculated using the equilibrium constants (Figure 6) point to the dominance of the neutral [Pb(**do2pa**)] and [Pb(**Me-do2pa**)] complexes in a wide range of intermediate pH, while monoprotonated complexes exist in small amounts in acidic pH. Free Pb^{2+} cation is only present in solution with significant concentrations below pH 4−5, while at high pH monohydroxo complexes are formed presumably due to deprotonation of a weakly coordinated water molecule.

The thermodynamic stability of the bismuth(III) complexes of H_2**do2pa** and H_2**Me-do2pa** could not be determined by potentiometric titrations. Indeed, the complexation of Bi^{3+} is usually hindered by the formation of a variety of bismuth(III) hydroxides from very low pH that may only be overcome if a fast and complete formation is achieved at low pH, which in turn prevents the determination of formation constants. The problems found were different for H_2**do2pa** and H_2**Me-do2pa**, as the bismuth(III) complex of H_2**Me-do2pa** was fully formed in the pH range useful for potentiometry (pH 2−12), while for H_2**do2pa** there was unavoidable precipitation at low pH due to a somewhat incomplete complex formation. Thus, potentiometric titrations in the presence of Bi^{3+} were performed only for H_2**Me-do2pa** in order to determine the potential formation of protonated species of the complex, while analogous experiments were not possible for H_2**do2pa**. Alternatively, spectrophotometric titrations at very high pH were used to determine the stability constants of the complexes, taking advantage of the fact that these complexes dissociate slowly in the presence of a very high concentration of hydroxide to yield essentially the bismuth(III) hydroxocomplexes $Bi(OH)_4^-$. This competition method for the determination of stability constants of bismuth(III) complexes has been successfully established in the literature,[50] and recently was also used by us.[21] The competition titrations were performed using a batch (out-of-cell) method at pH > 11 in aqueous medium with an ionic strength of 0.50 M in KCl, similarly to the conditions used in all potentiometric determinations, and equilibrium was attained after 2 weeks of incubation. Dissociation of the bismuth(III) complexes of both ligands was significant at high pH, which allowed for determination of stability constants. The results

DOI: 10.1021/acs.inorgchem.5b01079
Inorg. Chem. 2015, 54, 7045−7057

Table 3. Calculated pM Values[a] at pH 7.4 for the Complexes of H_2dodpa and H_2Me-dodpa, and for Related Compounds

metal ion	H_2**do2pa**	H_2**Me-do2pa**	H_2bp12c4	H_4dota	H_2ba12c4	H_2do2a
Pb^{2+}	10.47	12.83	15.0	18.4	10.0	12.1
Bi^{3+}	26.0	28.6		27.0		

[a]Calculated for 100% excess of ligand with $[M^{2+}]_{tot} = 1.0 \times 10^{-5}$ M, based on the reported stability constants.

obtained were best fitted to a speciation model containing BiL and BiL(OH) complexes for both ligands, as well as the competing $Bi(OH)_3$ and $Bi(OH)_4^-$ species, for which accurate stability constant values are available in the literature.[6] The stability constant obtained for [Bi(**Me-do2pa**)]$^+$ is very high, being significantly higher than the one reported for [Bi(dota)]$^-$.[17] The stability constant for [Bi(**do2pa**)]$^+$, while being more than 2 log units lower than that for [Bi(**Me-do2pa**)]$^+$, is still higher than that of [Bi(dota)]$^-$. Species distribution diagrams for the bismuth(III) complexes of H_2**Me-do2pa** and H_2**do2pa** were also plotted and are given in Figure S3 (Supporting Information). In the intermediate range of pH, the complexes exist exclusively in the form of the $(BiL)^+$ species, while the BiL(OH) species forms significantly above pH 10. It is only above pH 12 that dissociation of the complexes takes place, thus proving the excellent stability of these bismuth(III) complexes.

Thermodynamic stability constants alone are not adequate values to compare the ability to sequester a given metal cation by ligands of different basicity, as the complexation reaction of protonated ligands in solution is a competition between protons and the metal cation for the ligand. Conditional stability constants or more frequently pM values, defined as $-\log[M^{m+}]_{free}$, give a more accurate picture of the amount of complex formed at a given pH, and so allow a more straightforward comparison of different ligands. Therefore, pM values were obtained at physiological pH (7.4) for the studied complexes and related ones taking into account the stability constant values of Table 2. The results are collected in Table 3.

The pPb values obtained for H_2**do2pa** and H_2**Me-do2pa** are smaller than the corresponding value for H_4dota. However, the pBi value obtained for H_2**Me-do2pa** is the largest among the discussed ligands, being about two log units larger than that of H_4dota, while the pBi value for H_2**do2pa** is almost as high as that for H_4dota. These results prove that dipicolinate cyclen derivatives have very strong affinity for bismuth(III), notably in the case of H_2**Me-do2pa**, and such behavior is very encouraging for the use of bismuth(III) complexes for medical purposes. Nonetheless, a high thermodynamic stability of the complexes is only one of the crucial properties for medical applications, as the kinetic properties of the complexes are also very important.

Formation and Dissociation Kinetics of the Bismuth(III) and Lead(II) Complexes. A fast formation of the metal complexes is essential for their use as radiopharmaceuticals, as even very stable complexes may be useless if their formation requires rather harsh conditions to achieve a near quantitative complex formation (typically very high temperature and/or high pH), given that such conditions are impractical when working with most of the radioisotopes used in medicine. For this reason, it is important to know the formation rates of the lead(II) and bismuth(III) complexes investigated here.

The kinetics of bismuth(III) complexation were determined for H_2**do2pa** and H_2**Me-do2pa** by UV absorption spectroscopy in buffered aqueous media at 25 °C, under pseudo-first-order conditions in an excess of ligand (Table 4). Due to the extremely easy hydrolysis of the Bi^{3+} cation in aqueous solutions at pH ≥ 1, the coordinating buffers citrate (pH 3.0) and acetate (pH 5.0) were selected as appropriate media to ensure the solubility of the cation during the complexation assays. The complexation reaction was monitored by following the absorption bands of the complexes observed at ∼330−350 nm, which are likely related to metal-centered transitions involving the s and p orbitals of Bi^{3+}.[51] In the case of H_2**Me-do2pa**, the complexation process was found to be very fast at pH 5 (acetate buffer), being complete in less than 2 min (Figure S4 in the Supporting Information). Furthermore, it was still fast at pH 3 (citrate buffer) with a half-time formation of 12.5 min, with complexation being finished after about 1 h (Figure 7).[21] For H_2**do2pa**, the complexation rate is significantly slower at pH 5 (acetate buffer) with a half-time formation of 279 min (Figure S5 in the Supporting Information), while it is almost insignificant at pH 3 (citrate buffer). Similar assays performed for comparison with H_4dota showed that while bismuth(III) complexation is quite fast at pH 5, as it is complete after 5 min, it is contrastingly much slower at pH 3 with a formation half-time of 327 min (Figures S6 and S7 in the Supporting Information). The results obtained for H_2**Me-do2pa** are particularly promising, considering that bismuth(III) complexation is achieved at a much faster rate than with H_4dota at pH 3. However, H_2**do2pa** exhibits slow bismuth(III) complexation rates even at the highest pH investigated.

Table 4. Determined Half-Times (in min) of Formation for the Bismuth(III) Complexes of H_2do2pa, H_2Me-do2pa, and H_4dota at 25 °C in Buffered Aqueous Solutions

buffer	H_2**do2pa**	H_2**Me-do2pa**	H_4dota
acetate, pH 5	279	<2[a]	<5[a]
citrate, pH 3		12.5	327

[a]The time corresponds to approximately full formation; a half-time could not be determined.

The kinetics of lead(II) complexation were also studied by absorption spectroscopy in buffered aqueous media at 25 °C under pseudo-first-order conditions. However, as the weak absorptions of these complexes in the UV range were found to be invariably obstructed by the stronger absorption of the picolinate moieties of the ligands and of the buffering media, an indirect method was applied making use of the complexometric indicator Arsenazo III. The lead(II) complexes of H_2**do2pa** and H_2**Me-do2pa** were found to form slowly at acidic pH; thus, complexation was only studied in HEPES buffer at pH 7.4 (Figure S8 in the Supporting Information). Under such conditions, a formation half-time of 13.8 min was found for the H_2**Me-do2pa** complex, while for H_2**do2pa** the complexation is considerably slower, taking several hours. The complexation of Pb^{2+} by H_2**Me-do2pa** was also checked by ^{1}H NMR. Spectra were performed at pH 6.5 with equimolar concentrations of $PbCl_2$ and H_2**Me-do2pa**. The signals of free H_2**Me-do2pa** could not be observed after only 2 min, thus

DOI: 10.1021/acs.inorgchem.5b01079
Inorg. Chem. 2015, 54, 7045−7057

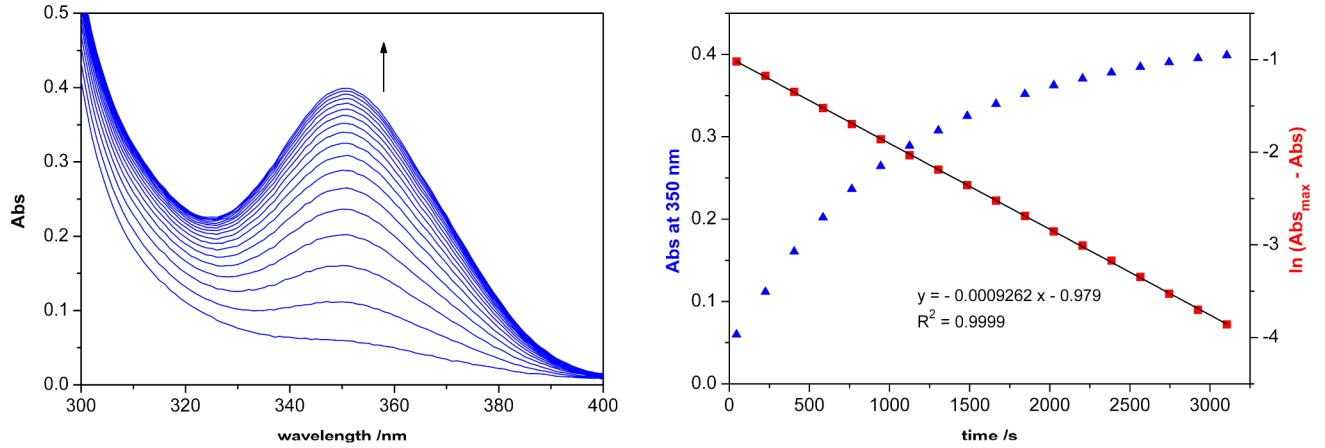

Figure 7. Time course of the UV spectra of a solution of Bi^{3+} in the presence of 10 equiv of H_2**Me-do2pa** at 25 °C and pH 3 in citrate buffer: spectra obtained at 3 min intervals (left); plot of the absorbance at 350 nm versus time and fit to obtain the first order rate constant (right).

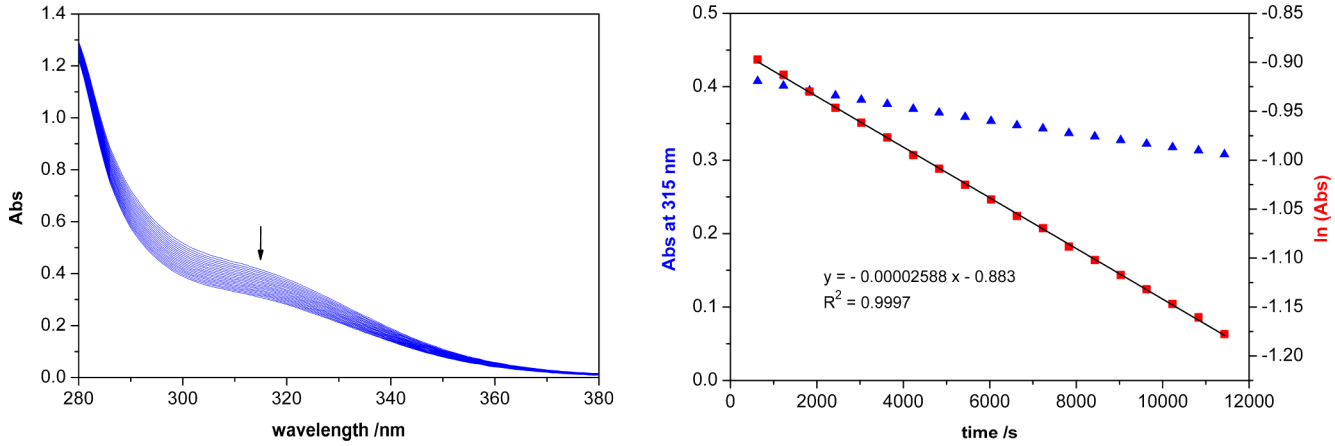

Figure 8. Time course of the UV spectra of [Pb(**Me-do2pa**)] in HEPES buffer at pH 7.4 and 25.0 °C with 100 equiv of K_2H_2edta: spectra obtained at 10 min intervals (left); absorbance at 315 nm versus time, and its fitting to obtain the observed first order rate constant (right).

demonstrating the fast complexation of Pb^{2+} by H_2**Me-do2pa** (Figure S9 in the Supporting Information).

The inertness of the complexes is also very important to ensure that after complexation the potentially toxic metal cations are not released. The dissociation kinetics of the bismuth(III) and lead(II) complexes were thus also investigated. The dissociation of the bismuth(III) complexes was followed by UV spectrophotometry at 25 °C in 1 M HCl aqueous solution. The half-life times determined were 23.9 min for H_2**Me-do2pa**[21] and 12.1 min for H_2**do2pa**. For comparison, the half-life time of the bismuth(III) complex of H_4dota was determined under the same conditions to be 22.7 min (Figures S10, S11, and S12 in the Supporting Information). Again, H_2**Me-do2pa** proves to be better than H_4dota regarding complex inertness, while the complex of H_2**do2pa** is significantly less inert than the other two. For lead(II) complexes, it is usual to observe rather fast dissociation kinetics in very acidic media. This was confirmed by following the dissociation of [Pb(**Me-do2pa**)] by ^{1}H NMR in 0.1 M DCl, as the complex was found to be totally dissociated after 7 min (Figure S13 in the Supporting Information). For this reason, a challenge test with 100 equiv of K_2H_2edta at pH 7.4 (HEPES buffer) was used instead to assess the inertness of the [Pb(**Me-do2pa**)] complex (Figure 8). Under such conditions, a half-life time of 446 min could be estimated, highlighting the excellent resistance of [Pb(**Me-do2pa**)] to transchelation.

CONCLUSIONS

In this work, we have shown that two cyclen based macrocycles bearing picolinate pendant arms, H_2**do2pa** and H_2**Me-do2pa**, present a high affinity for both Pb^{2+} and Bi^{3+} cations. A new, very convenient, three-step synthesis of the H_2**do2pa** ligand based on bisaminal chemistry has been developed starting from cyclen. A combination of X-ray diffraction experiments, NMR spectroscopy, and DFT calculations revealed that the [Pb(**Me-do2pa**)] and [Bi(**Me-do2pa**)]$^+$ complexes exist as the $\Delta(\delta\delta\delta\delta)/\Lambda(\lambda\lambda\lambda\lambda)$ enantiomeric pair both in the solid state and in solution. Furthermore, while the complex of Bi^{3+} presents a very rigid structure in solution, the Pb^{2+} analogue presents a fluxional behavior that has been attributed to the $\Delta(\delta\delta\delta\delta) \leftrightarrows \Lambda(\lambda\lambda\lambda\lambda)$ interconversion process.

The thermodynamic stability of the lead(II) complexes of H_2**do2pa** and H_2**Me-do2pa** is reasonably high, as evaluated by the corresponding pPb values, but still lower than that of the complex with H_4dota. However, our results point to an outstanding affinity of the ligands for bismuth(III), especially H_2**Me-do2pa**, when compared to related ligands such as H_4dota. Kinetic studies by ^{1}H NMR and UV−visible spectroscopy evidenced a very fast complexation of both metal ions by H_2**Me-do2pa**. Similar spectroscopic methods were also used to prove the very good inertness of the bismuth(III) complex of

DOI: 10.1021/acs.inorgchem.5b01079
Inorg. Chem. 2015, 54, 7045−7057

H_2**Me-do2pa** in acidic medium, while the lead(II) complex is very inert with regard to transchelation.

Given the overall favorable coordination properties of H_2**do2pa** and particularly H_2**Me-do2pa** as chelators for lead(II) and bismuth(III), their use as ligands for applications in α-radioimmunotherapy can be envisaged. Taking into account that the H_2**Me-do2pa** complexes presented the best behavior, coupling the ligand to targeting biomolecules via one of the nitrogen atoms can be easily considered. Efforts are currently in progress to develop new BCAs based on the H_2**Me-do2pa** framework, essentially for radiolabeling with ^{213}Bi.

EXPERIMENTAL SECTION

General Methods. Reagents were purchased from ACROS Organics and from Aldrich Chemical Co. Cyclen was purchased from Chematech (Dijon, France). Cyclen-glyoxal (**2**)[25] and 6-chloromethylpyridine-2-carboxylic acid methyl ester (**3**)[28] were synthesized as previously described. Elemental analyses were performed at the Service de Microanalyse, CNRS, 69360 Solaize, France. NMR and mass spectra were recorded at the "Services communs" of the University of Brest. The HR-MS analyses were performed at the Institute of Analytic and Organic Chemistry, ICOA, in Orleans. ^{1}H and ^{13}C NMR spectra were recorded with Bruker Avance 500 (500 MHz), Bruker Avance 400 (400 MHz), or Bruker AMX-3 300 (300 MHz) spectrometers. MALDI mass spectra were recorded with an Autoflex MALDI TOF III LRF200 CID spectrometer, while high resolution ESI-TOF mass spectra were recorded using a LC-Q-q-TOF Applied Biosystems QSTAR Elite spectrometer in the positive mode.

Compound 4. To a solution of compound **2** (0.499 g, 2.57 mmol) and NaI (1.54 g, 10.28 mmol) in dry CH_3CN (15 mL) was added dropwise a solution of **3** (1.00 g, 5.39 mmol) in the same solvent (10 mL). The mixture was stirred at room temperature for 9 days. The white precipitate formed was isolated by filtration, washed with CH_3CN (3 × 5 mL) and diethyl ether (3 × 5 mL), and dried under a vacuum to give 1.79 g of **4** (93%) as a white solid. δ_C ppm (solvent D_2O, 298 K, 75.5 MHz): 45.9 (C-py); 49.3, 59.8, 63.7, 64.7 (CH_2−N); 56.4 (−OCH_3), 80.4 (C−H), 129.7, 134.0, 143.2, 150.6, 150.9 (Py), 169.2 (CO).

H_2do2pa. Compound **4** (1.68 g, 2.24 mmol) was dissolved in hydrazine monohydrate (13 mL), and the mixture was heated to reflux overnight. The mixture was evaporated, and the crude product was taken up with water (20 mL) and washed with chloroform (4 × 20 mL). The aqueous phase was evaporated. Addition of absolute ethanol resulted in the precipitation of insoluble salts, which were removed by filtration. The filtrate was evaporated to give a yellowish powder that was dissolved in 6 M HCl (30 mL), and the solution was heated to 80 °C for 24 h, filtrated, and concentrated to dryness. Addition of methanol resulted in the formation of a precipitate that was isolated by filtration and dried under a vacuum to give 0.981 g of H_2**do2pa**·5HCl as a yellow solid (85%). Anal. Calcd for $C_{22}H_{30}N_6O_4$·5HCl·4H_2O: C, 37.92; H, 6.22; N, 12.06%. Found: C, 37.75; H, 6.28; N, 12.04%. δ_H ppm (solvent D_2O, 295 K, 500 MHz, pD 0.7): 7.75 (m, 2 H, py); 7.59 (d, 2 H, py, ^3J = 7.6 Hz); 7.37 (d, 2 H, py, ^3J = 7.8 Hz); 4.05 (s, 4 H, —CH_2—); 3.37 (b, 4 H, —CH_2—); 3.27 (b, 4 H, —CH_2—); 3.11 (b, 4 H, —CH_2—); 2.90 (b, 4 H, —CH_2—). δ_C (solvent D_2O, 295 K, 125.8 MHz, pD 0.7): 42.6, 48.8, 55.2 (secondary C); 123.9, 126.3, 137.6 (tertiary C); 145.3, 158.4, 167.0 (quaternary C). IR: 1692 ν(C=O), 1462 $\nu(C{=}N)_{py}$ cm^{-1}. MS (ESI$^+$): m/z 443 ([$C_{22}H_{31}N_6O_4$]$^+$), 222 ([$C_{22}H_{32}N_6O_4$]$^{2+}$).

[Bi(do2pa)](NO$_3$). H_2**do2pa**·5HCl·4H_2O (58.0 mg, 0.083 mmol) was dissolved in 3 mL of H_2O, and $Bi(NO_3)_3$·5H_2O (53.5 mg, 1.3 equiv) was added. The mixture (pH 1) was stirred at room temperature for 30 min. The pH was raised to pH 4 by addition of aqueous KOH, which resulted in the formation of a white precipitate. The resulting mixture was stirred for 16 h under reflux. The reaction mixture was cooled down to room temperature, and MeOH was added. The precipitate was filtered off, and the filtrate was evaporated and washed several times with a mixture of MeOH/acetone to give 55.0 mg (93%) of [Bi(**do2pa**)](NO$_3$) as a pale yellow solid. δ_H ppm (solvent D_2O, 298 K, 300 MHz): 2.85 (t, 2 H, −CH_2−), 3.29 (d, 2 H, −CH_3), 3.56 (m, 10 H, −CH_2−), 4.00 (d, 2 H), 4.80 (d, 2 H, −CH_2−py), 4.94 (d, 2 H, −CH_2−py, ^2J = 16.8 Hz), 7.92 (d, 2 H, ^3J = 7.9 Hz, py), 8.05 (d, 2 H, ^3J = 7.8 Hz, py), 8.30 (t, 2 H, ^3J = 7.8 Hz, py). δ_C (solvent D_2O, 298 K, 125.8 MHz): 48.48, 49.27, 55.51, 59.30, 63.10 (secondary C); 128.50, 130.02, 144.39 (tertiary C); 152.77, 157.71, 174.03 (quaternary C). HRMS: m/z found 649.1967, calcd $C_{22}H_{28}BiN_6O_4$ (M$^+$) 649.1971.

[Bi(Me-do2pa)](NO$_3$). The preparation of this compound followed the same procedure as that described for [Bi(**do2pa**)](NO$_3$) by using H_2**Me-do2pa**·4HCl (28.0 mg, 0.045 mmol) and $Bi(NO_3)_3$·5H_2O (22 mg) in 3 mL of water (yield 32 mg, 82%). δ_H ppm (solvent D_2O, 298 K, 300 MHz): 2.38 (s, 6 H, −CH_3), 2.99−3.47 (m, 12 H, −CH_2−), 3.60 (m, 4 H, −CH_2−), 4.86 (q, 4 H, −CH_2−py), 7.96 (d, 2 H, ^3J = 7.4 Hz, py), 8.04 (d, 2 H, ^3J = 7.4 Hz, py), 8.32 (t, 2 H, ^3J = 7.4 Hz, py). δ_C ppm (solvent D_2O, 298 K, 125.8 MHz): 46.65, 51.77 (primary C); 53.49, 55.94, 57.53, 59.61, 62.12 (secondary C); 129.39, 130.75, 145.47 (tertiary C); 151.55, 158.96, 174.00 (quaternary C). HRMS: m/z found 677.2280, calcd $C_{24}H_{32}BiN_6O_4$ (M$^+$) 677.2284.

[Pb(do2pa)]. H_2**do2pa**·5HCl·4H_2O (52 mg, 0.075 mmol) was dissolved in 3 mL of water, and $PbCl_2$ (30 mg, 1.4 equiv) was added to the solution followed by a few drops of concentrated HCl until complete dissolution of $PbCl_2$. The solution was stirred at room temperature for 30 min. The pH was raised to pH 7 by addition of KOH. The resulting mixture was stirred for 16 h under reflux. The reaction mixture was cooled down to room temperature, and MeOH was added. The precipitate was filtered off. The filtrate was evaporated and washed several times with MeOH to yield 50 mg (90%) of [Pb(**do2pa**)] as a pale yellow solid. δ_H ppm (solvent D_2O, 298 K, 300 MHz): 2.99 (m, 4 H, −CH_2−), 3.24 (m, 8 H, −CH_2−), 3.51 (m, 4 H, −CH_2−), 4.47 (s, 4 H, −CH_2−py), 7.57 (d, 2 H, ^3J = 7.9 Hz, py), 7.88 (d, 2 H, ^3J = 7.8 Hz, py), 7.99 (t, 2 H, ^3J = 7.8 Hz, py). δ_C (solvent D_2O, 298 K, 125.8 MHz): 46.53, 48.11, 48.21, 56.25, 62.23 (secondary C); 126.34, 128.35, 142.02 (tertiary C); 158.23, 158.59, 174.05 (quaternary C). HRMS: m/z found 325.1049, calcd $C_{22}H_{30}N_6O_4Pb$ (MH_2^+) 325.1043.

[Pb(Me-do2pa)]. The preparation of this compound followed the same procedure as that described for [Pb(**do2pa**)] by using H_2**Me-do2pa**·4HCl (59 mg, 0.10 mmol) and $PbCl_2$ (22 mg) in 3 mL of water (yield 72 mg, 100%). δ_H ppm (solvent D_2O, 298 K, 300 MHz): 2.18 (s, 6 H, −CH_3), 2.50−3.60 (sm, 16 H, −CH_2−), 4.45 (bs, 4 H, −CH_2−py), 7.70 (d, 2 H, ^3J = 7.1 Hz, py), 7.88 (d, 2 H, ^3J = 7.7 Hz, py), 7.99 (t, 2 H, ^3J = 7.7 Hz, py). δ_C (solvent D_2O, 298 K, 125.8 MHz): 42.48 (primary C); 59.12 (secondary C); 123.77, 125.57, 139.23 (tertiary C); 151.60, 156.37, 171.67 (quaternary C). HRMS: m/z found 677.2320, calcd $C_{24}H_{33}N_6O_4Pb$ (MH$^+$) 677.2330.

Single Crystal X-ray Diffraction Measurements. Single-crystal X-ray diffraction data were collected at 170 K on an X-CALIBUR-2 CCD 4-circle diffractometer (Oxford Diffraction) with graphite-monochromatized Mo Kα radiation (λ = 0.71073). Crystal data and structure refinement details are given in Table 5. Unit-cell determination and data reduction, including interframe scaling, Lorentz, polarization, empirical absorption, and detector sensitivity corrections, were carried out using attached programs of Crysalis software (Oxford Diffraction).[52] Structures were solved by direct methods and refined by the full matrix least-squares method on F^2 with the SHELXL[53] suites of programs. The hydrogen atoms were identified at the last step and refined under geometrical restraints and isotropic U-constraints.[54] CCDC numbers 1058057 and 1049922 contain the supplementary crystallographic data for this paper. These data can be obtained free of charge from the Cambridge Crystallographic Data Centre via www.ccdc.cam.ac.uk/data_request/cif.

Computational Methods. All calculations were performed employing DFT within the hybrid meta generalized gradient approximation (hybrid meta-GGA), with the TPSSh exchange-correlation functional,[55] and the Gaussian 09 package (revision A.02).[56] Full geometry optimizations of the [Pb(**Me-do2pa**)] and [Bi(**Me-do2pa**)]$^+$ systems were performed in water solution by using

DOI: 10.1021/acs.inorgchem.5b01079
Inorg. Chem. 2015, 54, 7045−7057

Table 5. Crystal Data and Refinement Details for $4\cdot 3H_2O$ and $[Pb(Me\text{-}do2pa)]\cdot 6H_2O$

	$4\cdot 3H_2O$	$[Pb(\mathbf{Me\text{-}do2pa})]\cdot 6H_2O$
formula	$C_{26}H_{40}I_2N_6O_7$	$C_{24}H_{44}N_6O_{10}Pb$
MW	802.44	783.84
crystal system	monoclinic	monoclinic
space group	$P2_1/c$	$c2/c$
T (K)	170(2)	297(2)
a (Å)	12.5519(3)	12.5172(3)
b (Å)	18.4030(4)	17.9162(5)
c (Å)	14.2774(4)	13.4738(3)
β (deg)	106.503(3)	91.451(2)
V (Å^3)	3162.11(14)	3020.67(13)
F(000)	1600	1568
Z	4	4
λ (Å) (Mo Kα)	0.71073	0.71073
D_{calc} (g cm^{-3})	1.686	1.724
μ (mm^{-1})	2.040	5.647
θ range (deg)	2.92−28.28	3.02−26.37
R_{int}	0.0413	0.0355
reflns measd	27739	11434
unique reflns	7851	3093
reflns obsd	5426	2841
GOF on F^2	0.856	1.145
R1[a]	0.0306	0.0274
wR2 (all data)[b]	0.0591	0.0705
largest differences peak and hole (e Å^{-3})	1.044 and −0.474	1.612 and −0.442

[a] $R1 = \sum||F_0| - |Fc||/\sum|F_o|$. [b] $wR2 = \{\sum[w(|F_0|^2 - |Fc|^2)^2]/\sum[w(F_0^4)]\}^{1/2}$.

the relativistic effective core potentials of Dolg et al. (ECP60MDF, 60 core electrons) and the associated (12s12p9d3f2g)/[6s6p4d3f2g] valence basis set for Pb and Bi,[57] and the 6-31G(d) basis set for C, H, N, and O atoms. This ECP was shown to provide good results for both Pb and Bi complexes with N and O donor atoms.[58] No symmetry constraints have been imposed during the optimizations. The default values for the integration grid ("fine") and the SCF energy convergence criteria (10^{-8}) were used. The stationary points found on the potential energy surfaces as a result of the geometry optimizations have been tested to represent energy minima rather than saddle points via frequency analysis. Solvent effects were evaluated by using the polarizable continuum model (PCM), in which the solute cavity is built as an envelope of spheres centered on atoms or atomic groups with appropriate radii. In particular, we used the integral equation formalism (IEFPCM) variant as implemented in Gaussian 09.[59] In aqueous solution, relative free energies of the different isomers include non-potential-energy contributions (zero point energies and thermal terms) obtained through frequency analysis. The ring inversion process of $[Pb(\mathbf{Me\text{-}do2pa})]$ was investigated in aqueous solution by means of the synchronous transit-guided quasi-Newton method.[60] The nature of the saddle points and intermediates was characterized by frequency analysis. The relative energy barriers calculated include nonpotential energy contributions (that is, zero point energies and thermal terms) obtained by frequency analysis.

The NMR shielding tensors of $[Bi(\mathbf{Me\text{-}do2pa})]^+$ were calculated in aqueous solution using the TPSSh functional and the GIAO method.[61] In these calculations, we employed the EPR-III basis set of Barone[62] for C, H, N, and O atoms, which is a triple-ζ basis set including diffuse functions, double d-polarizations, and a single set of f-polarization functions, together with an improved s-part to better describe the nuclear region. For ^{13}C NMR chemical shift calculation purposes, the NMR shielding tensors of CH_4 were calculated at the TPSSh/EPR-III level. Chemical shifts were subsequently obtained by using the experimental δ value for gas phase methane (−7.0 ppm).[63]

Thermodynamic Stability Studies. The setup for potentiometric titrations has been described before.[64] The titrant was a carbonate-free KOH solution at ca. 0.50 M prepared from a commercial ampule of analytical grade, and the exact concentration was obtained by application of Gran's method[65] upon titration of a standard HNO_3 solution. Stock solutions of the ligands were prepared at ca. 2×10^{-3} M. An analytical solution of $Pb(NO_3)_2$ was prepared at ca. 0.05 M in water, while an analytical solution of $Bi(NO_3)_3$ was instead prepared at 0.025 M in 1 M aqueous HCl to avoid metal hydrolysis. Both metal solutions were standardized by complexometric titration against a standard K_2H_2edta (ethylenediaminetetracetic acid) solution.[66] Potentiometric titrations were run with ca. 0.04 mmol of ligand in a total volume of 30 mL, containing ca. 0.9 equiv of metal ions in the case of complexations, at 25.0 ± 0.1 °C and with the ionic strength kept at 0.50 ± 0.01 M using KCl as background electrolyte. The $[H^+]$ of the solutions was determined by measurement of the electromotive force of the cell, $E = E^0 + Q\log[H^+] + E_j$. The term pH is defined as $-\log[H^+]$, and a value of $K_w = [H^+][OH^-] = 10^{-13.72}$ was taken from the literature for our experimental conditions.[67] The terms E^0 and Q were determined by titration of a solution of known hydrogen-ion concentration at the same ionic strength. The liquid-junction potential, E_j, was found to be negligible under the experimental conditions used. Each titration consisted of 80−100 equilibrium points in the pH range 2.5−11.5, and at least two replicate titrations were performed for each individual system. The potentiometric data were refined with the Hyperquad software,[68] and speciation diagrams were plotted using the Hyss software.[69]

Spectrophotometric competition titrations were measured in a Unicam UV4 spectrophotometer at 25.0 ± 0.1 °C using a Huber CCE-K6 circulating thermostatic bath. Stock solutions of preformed bismuth(III) complexes of H_2**do2pa** and H_2**Me-do2pa** at neutral pH were prepared at ca. 2.0×10^{-3} M, by addition of the acidic solution of $Bi(NO_3)_3$ to an aqueous solution of each ligand (in exact 1:1 molar ratio) followed by very slow neutralization of the mixture with aqueous KOH solution under constant heating (80−90 °C). Each batch titration consisted of a set of 12 individual points distributed in the estimated pH range 11.4−12.6 for H_2**do2pa** or 12.0−13.3 for H_2**Me-do2pa**, prepared under a nitrogen atmosphere and kept in tightly sealed vials. Individual points were prepared by addition of precise volumes of a titrant KOH solution of accurately known concentration (at ca. 0.50 M for H_2**Me-do2pa** and ca. 0.10 M for H_2**do2pa**) to a mixture of the preformed complex solution containing ca. 2×10^{-3} mmol of complex and a concentrated KCl solution to keep each sample at 0.50 M in KCl. The vials were thermostatized at 25 °C until the points attained equilibrium, which happened after 2 weeks. The pH of these points was not measured, but the value of $[H^+]$ was instead calculated by the program from the experimental data. UV absorbance spectra were measured after quick transfer of each sample solution from its vial to a semimicro UV cuvette while avoiding contact with the atmosphere. Measurements used for the determinations were centered in the absorption band of each complex (335 nm for $[Bi(\mathbf{do2pa})]^+$ and 350 for $[Bi(\mathbf{Me\text{-}do2pa})]^+$), and the molar absorptivity of the ML species was used as determined from the stock solutions of preformed complexes. The spectroscopic data were refined with the HypSpec software,[70] assuming a model containing the species BiL and BiLOH for both ligands, as well as the competing $Bi(OH)_4^-$ species. The formation constants of the $Bi(OH)_3$ and $Bi(OH)_4^-$ species used in the refinements were taken from the literature.[6]

The overall equilibrium (formation) constants β_{H_hL} and $\beta_{M_mH_hL_l}$ are defined by $\beta_{M_mH_hL_l} = [M_mH_hL_l]/[M]^m[H]^h[L]^l$ and $\beta_{MH_{-1}L} = \beta_{ML(OH)} \times K_w$, while stepwise equilibrium constants are given by $K_{M_mH_hL_l} = [M_mH_hL_l]/[M_mH_{h-1}L_l][H]$ and correspond to the difference in log units between overall constants of sequentially protonated (or hydroxide) species. The pM values for metal complexes were calculated from the full set of stability constants for each system at pH 7.4 with $C_L = 2.0 \times 10^{-5}$ M and $C_M = 1.0 \times 10^{-5}$ M.

Kinetic Determinations. UV spectra were measured using the spectrophotometer setup described above. The formation of the

DOI: 10.1021/acs.inorgchem.5b01079
Inorg. Chem. 2015, 54, 7045−7057

lead(II) and bismuth(III) complexes of H_2**do2pa**, H_2**Me-do2pa** and H_4dota was studied in buffered aqueous solutions at 25 °C. Stock solutions of potassium citrate (1 M, pH 3.0), potassium acetate (1 M, pH 5.0), and HEPES (0.5 M, pH 7.4) buffers were prepared in water. Stock solutions of $PbCl_2$ and $BiCl_3$ were prepared at 2.5×10^{-3} M in water or in aqueous 0.5 M HCl, respectively. A solution of Arsenazo III complexometric indicator was prepared at 1 mM in water. For bismuth(III), the increasing intensity of the UV absorption band of each complex (335 nm for [Bi(**do2pa**)]$^+$, 350 for [Bi(**Me-do2pa**)]$^+$, and 306 for [Bi(dota)]$^-$) was followed at pH 3.0 (500 mM citrate buffer) and pH 5.0 (500 mM acetate buffer), under pseudo-first-order conditions at $[L]_{tot} = 10 \times [Bi^{3+}]_{tot} = 1$ mM. For lead(II), an indirect method was applied using the Arsenazo III complexometric indicator. This indicator forms a weak complex with Pb^{2+}, displaying a band on the visible range (at ~655 nm) that disapears upon formation of the Pb^{2+} complex with the studied ligands. The decreasing band of the Pb^{2+}:indicator complex formed (1:1 ratio) was followed at pH 7.4 (100 mM HEPES buffer), under pseudo-first-order conditions with $[L]_{tot} = 10 \times [Bi^{3+}]_{tot} = 0.5$ mM.

The acid-assisted dissociation of the bismuth(III) complexes of H_2**do2pa**, H_2**Me-do2pa**, and H_4dota was studied under pseudo-first-order conditions at 25 °C in 1 M HCl. Concentrated acid was added to sample solutions containing the preformed complex with a starting complex concentration of 0.13 mM. The reaction was followed by the decreasing intensity of the UV absorption of the complex (360 nm for H_2**Me-do2pa**), or the increasing UV absorption of uncomplexed Bi^{3+} in chloride medium (322 nm for H_2**do2pa** and H_4dota). The dissociation of the [Pb(**Me-do2pa**)] complex was studied by challenge with excess of K_2H_2edta at pH 7.4. The decreasing intensity of the UV absorption of the complex (315 nm) was followed at $[H_4edta]_{tot} = 100 \times$ [Pb(**Me-do2pa**)] = 20 mM in 200 mM HEPES buffer.

■ ASSOCIATED CONTENT

Supporting Information

View of the crystal structure of [H_2**Me-do2pa**]·2HCl·5H_2O; crystal data and refinement details for H_2**Me-do2pa**·2HCl·5H_2O; calculated ^{13}C NMR chemical shifts of the four isomers at the TPSSh/ECP60MDF/EPR-III level; overall protonation constants (log β_{HhL}) of **do2pa**$^{2-}$ and **Me-do2pa**$^{2-}$ and overall stability constants (log β_{MHhL}) of their complexes with Pb^{2+} and Bi^{3+} metal ions; species distribution diagrams of aqueous solutions of H_2**do2pa** and H_2**Me-do2pa**; species distribution diagram of bismuth(III) in the presence of H_2**Me-do2pa** and H_2**do2pa**; kinetic plots for the formation and dissociation of lead(II) and bismuth(III) complexes; ^{1}H NMR spectra of H_2**Me-do2pa** after addition of Pb^{2+}; ^{1}H NMR spectra [Pb(**Me-do2pa**)] before addition and after addition of 0.1 M DCl. The Supporting Information is available free of charge on the ACS Publications website at DOI: 10.1021/acs.inorgchem.5b01079.

■ AUTHOR INFORMATION

Corresponding Authors

*E-mail: delgado@itqb.unl.pt.
*E-mail: carlos.platas.iglesias@udc.es.
*E-mail: Raphael.Tripier@univ-brest.fr.

Notes

The authors declare no competing financial interest.

■ ACKNOWLEDGMENTS

R.T. acknowledges the Ministère de l'Enseignement Supérieur et de la Recherche, the Centre National de la Recherche Scientifique, the ANR program BIBICHEMAP, the UEB "RTR Biologie-Santé", and especially the *Conseil Général du Finistère* (L.M.P.L. financial support). R.T. also thanks the "Service Commun" of NMR facilities of the University of Brest and Mariane Le Fur, Roxanne Ménard, and Zineb Liraki for their participation in the preliminary works. C.P.-I. is indebted to Centro de Supercomputación de Galicia (CESGA) for providing the computer facilities. R.D. and L.M.P.L. acknowledge Fundação para a Ciência e a Tecnologia (FCT) for the financial support under Project PTDC/QEQ-SUP/2718/2012. L.M.P.L. thanks FCT also for a postdoctoral fellowship (SFRH/BPD/73361/2010).

■ REFERENCES

(1) (a) Hassfjell, S.; Brechbiel, M. W. *Chem. Rev.* **2001**, *101*, 2019−2036. (b) Brechbiel, M. W. *Dalton Trans.* **2007**, 4918−4928. (c) Couturier, O.; Supiot, S.; Degraef-Mougin, M.; Faivre-Chauvet, A.; Carlier, T.; Chantal, J.-F.; Davodeau, F.; Cherel, M. *Eur. J. Med. Mol. Imaging* **2005**, *32*, 601−614.

(2) Bartos, B.; Lyczko, K.; Kasperek, A.; Krajewski, S.; Bilewicz, A. *J. Radioanal. Nucl. Chem.* **2013**, *295*, 205−209.

(3) Price, E. W.; Orvig, C. *Chem. Soc. Rev.* **2014**, *43*, 260−290.

(4) Yong, K.; Brechbiel, M. W. *Dalton Trans.* **2011**, *40*, 6068−6076.

(5) Montavon, G.; Le Du, A.; Champion, J.; Rabung, T.; Morgenstern, A. *Dalton Trans.* **2012**, *41*, 8615−8623.

(6) Cukrowsky, I.; Hancock, R. D.; Luckay, R. C. *Anal. Chim. Acta* **1996**, *319*, 39−48.

(7) (a) Baidoo, K. E.; Milenic, D. E.; Brechbiel, M. W. *Nucl. Med. Biol.* **2013**, *40*, 592−599. (b) Ramogida, C. F.; Orvig, C. *Chem. Commun.* **2013**, *49*, 4720−4739.

(8) Cuenot, F.; Meyer, M.; Espinosa, E.; Guilard, R. *Inorg. Chem.* **2005**, *44*, 7895−7910.

(9) Goyer, R. A. In *Handbook on Toxicity of Inorganic Compounds*; Seiler, H. G., Sigel, A., Sigel, H., Eds.; Marcel Dekker: New York, 1988; pp 359−382.

(10) (a) Da Costa, C. P.; Rigel, H. *Inorg. Chem.* **2000**, *39*, 5985−5993. (b) Martin, R. B. *Inorg. Chim. Acta* **1998**, *283*, 30−36. (c) Magyar, J. S.; Weng, T.-C.; Stern, Ch. M.; Dye, D. F.; W. Rous, B.; Payne, J. C.; Bridgewater, M. A.; Mijovilovich, B.; Parkin, G.; Zaleski, J. M.; Penner-Hahn, J. E.; Godwin, H. A. *J. Am. Chem. Soc.* **2005**, *127*, 9495−9505. (d) Sigel, H.; Da Costa, C. P.; Martin, R. B. *Coord. Chem. Rev.* **2001**, *219−221*, 435−461. (e) Sigel, B. E.; Fischer, H.; Farkas, E. *Inorg. Chem.* **1983**, *22*, 925−934. (f) Tajimir-Riahi, H. A.; Langlais, M.; Savoie, R. *Nucleic Acids Res.* **1988**, *16*, 751−762. (g) Kazantis, G. In *Poisoning, Diagnosis and Treatment*; Vale, J. A., Meredith, T. J., Eds.; Update Books: London, 1981; pp 171−175. (h) Baltrop, D. In *Poisoning, Diagnosis and Treatment*; Vale, J. A., Meredith, T. J., Eds.; Update Books: London, 1981; pp 178−185.

(11) Briand, G. G.; Burford, N. *Chem. Rev.* **1999**, *99*, 2601−2657.

(12) (a) Hancock, R. D.; Maumela, H.; de Sousa, A. S. *Coord. Chem. Rev.* **1996**, *148*, 315−347. (b) Luckay, R.; Cukrowski, I.; Mashishi, J.; Reibenspies, J. H.; Bond, A. H.; Rogers, R. D.; Hancock, R. D. *J. Chem. Soc., Dalton Trans.* **1997**, 901−908.

(13) Maumela, H.; Hancock, R. D.; Carlton, L.; Reibenspies, J. H.; Wainwright, K. P. *J. Am. Chem. Soc.* **1995**, *117*, 6698−6707.

(14) Hancock, R. D.; Reibenspies, J. H.; Maumela, H. *Inorg. Chem.* **2004**, *43*, 2981−2987.

(15) Cuenot, F.; Meyer, M.; Espinosa, E.; Bucaille, A.; Burgat, R.; Guilard, R.; Marichal-Westrich, C. *Eur. J. Inorg. Chem.* **2008**, 267−283.

(16) Pippin, C. G.; Mcmurry, T. J.; Brechbiel, M. W.; McDonals, M.; Lambrecht, R.; Milenic, D.; Roselli, M.; Colcher, D.; Gansow, O. A. *Inorg. Chim. Acta* **1995**, *239*, 43−51.

(17) Csajbok, E.; Baranyai, Z.; Banyai, I.; Brucher, E.; Kiraly, R.; Muller-Fahrnow, A.; Platzek, J.; Raduchel, B.; Schafer, M. *Inorg. Chem.* **2003**, *42*, 2342−2349.

(18) Hassfjell, S.; Kongshaug, K. O.; Romming, C. *Dalton Trans.* **2003**, 1433−1437.

(19) Wang, X.; Zhang, X.; Lin, J.; Chen, J.; Xu, Q.; Guo, Z. *Dalton Trans.* **2003**, 2379−2380.

(20) (a) Morfin, J.-F.; Tripier, R.; Le Baccon, M.; Handel, H. *Inorg. Chim. Acta* **2009**, *362*, 1781−1786. (b) Morfin, J.-F.; Tripier, R.; Le Baccon, M.; Handel, H. *Polyhedron* **2009**, *28*, 3691−3698.

DOI: 10.1021/acs.inorgchem.5b01079
Inorg. Chem. 2015, 54, 7045−7057

(21) Lima, L. M. P.; Beyler, M.; Oukhatar, F.; Le Saec, P.; Faivre-Chauvet, A.; Platas-Iglesias, C.; Delgado, R.; Tripier, R. *Chem. Commun.* **2014**, *50*, 12371−12374.
(22) Ferreiros-Martinez, D.; Esteban-Gomez, A.; de Blas, C.; Platas-Iglesias, T.; Rodriguez-Blas. *Inorg. Chem.* **2009**, *48*, 11821−11831.
(23) Rodríguez-Rodríguez, A.; Esteban-Gómez, D.; De Blas, A.; Rodríguez-Blas, T.; Fekete, M.; Botta, M.; Tripier, R.; Platas-Iglesias, C. *Inorg. Chem.* **2012**, *51*, 2509−2521.
(24) Rodriguez-Rodriguez, A.; Garda, Z.; Ruscsák, E.; Esteban-Gómez, D.; de Blas, A.; Rodríguez-Blas, T.; Lima, L. M. P.; Beyler, M.; Tripier, R.; Tircsó, G.; Platas-Iglesias, C. *Dalton Trans.* **2015**, *44*, 5017−5031.
(25) Develay, E.; Tripier, R.; Chuburu, F.; Le Baccon, M.; Handel, H. *Eur. J. Org. Chem.* **2003**, *16*, 3047−3050.
(26) De León-Rodríguez, L. M.; Kovacs, Z.; Esqueda-Oliva, A. C.; Miranda-Olvera, A. D. *Tetrahedron Lett.* **2006**, *47*, 6937−6940.
(27) Le Baccon, M.; Chuburu, F.; Toupet, L.; Handel, H.; Soibinet, M.; Déchamps-Olivier, I.; Barbier, J.-P.; Aplincourt, M. *New J. Chem.* **2001**, *25*, 1168−1174.
(28) Mato-Iglesias, M.; Roca-Sabio, A.; Pálinkás, Z.; Esteban-Gómez, D.; Platas-Iglesias, C.; Tóth, É.; de Blas, A.; Rodríguez-Blas, T. *Inorg. Chem.* **2008**, *47*, 7840−7851.
(29) Pearson, R. G. *J. Am. Chem. Soc.* **1963**, *85*, 3533−3539.
(30) Rodriguez-Rodriguez, A.; Esteban-Gómez, D.; de Blas, A.; Rodríguez-Blas, T.; Botta, M.; Tripier, R.; Platas-Iglesias, C. *Inorg. Chem.* **2012**, *51*, 13419−13429.
(31) Nugent, J. W.; Lee, H.-S.; Reibenspies, J. H.; Hancock, R. D. *Polyhedron* **2015**, *91*, 120−127.
(32) Shimoni-Livny, L.; Glusker, J. P.; Bock, C. W. *Inorg. Chem.* **1998**, *37*, 1853−1867.
(33) Esteban-Gomez, D.; Platas-Iglesias, C.; Enriquez-Perez, T.; Avecilla, F.; de Blas, A.; Rodriguez-Blas, T. *Inorg. Chem.* **2006**, *45*, 5407−5416.
(34) Aime, S.; Botta, M.; Fasano, M.; Marques, M. P. M.; Geraldes, C. F. G. C.; Pubanz, D.; Merbach, A. E. *Inorg. Chem.* **1997**, *36*, 2059−2068.
(35) Corey, E. J.; Bailar, J. C., Jr. *J. Am. Chem. Soc.* **1959**, *81*, 2620−2629.
(36) Beattie, J. K. *Acc. Chem. Res.* **1971**, *4*, 253−259.
(37) Piguet, C.; Bünzli, J.-C. G.; Bernardinelli, G.; Bochet, C. G.; Froidevaux, P. *J. Chem. Soc., Dalton Trans.* **1995**, 83−97.
(38) (a) Regueiro-Figueroa, M.; Esteban-Gómez, D.; De Blas, A.; Rodríguez-Blas, T.; Platas-Iglesias, C. *Eur. J. Inorg. Chem.* **2010**, 3586−3595. (b) Regueiro-Figueroa, M.; Bensenane, B.; Ruscsák, E.; Esteban-Gómez, D.; Charbonnière, L. J.; Tircsó, G.; Tóth, I.; de Blas, A.; Rodríguez-Blas, T.; Platas-Iglesias, C. *Inorg. Chem.* **2011**, *50*, 4125−4141. (c) Lima, L. M. P.; Lecointre, A.; Morfin, J.-F.; de Blas, A.; Visvikis, D.; Charbonnière, L. J.; Platas-Iglesias, C.; Tripier, R. *Inorg. Chem.* **2011**, *50*, 12508−12521.
(39) Platas-Iglesias, C. *Eur. J. Inorg. Chem.* **2012**, 2023−2033.
(40) van Wüllen, C. *J. Chem. Phys.* **2012**, *136*, 114110.
(41) (a) Purgel, M.; Baranyai, Z.; de Blas, A.; Rodriguez-Blas, T.; Banyai, I.; Platas-Iglesias, C.; Toth, I. *Inorg. Chem.* **2010**, *49*, 4370−4382. (b) Fodor, T.; Banyai, I.; Benyei, A.; Platas-Iglesias, C.; Purgel, M.; Horvath, G. L.; Zekany, L.; Tircso, G.; Toth, I. *Inorg. Chem.* **2015**, *54*, 5426−5437.
(42) Ascenso, J. R.; Delgado, R.; Fraústo da Silva, J. J. R. *J. Chem. Soc., Perkin Trans. 2* **1985**, 781−788.
(43) (a) Mato-Iglesias, M.; Balogh, E.; Platas-Iglesias, C.; Tóth, E.; de Blas, A.; Rodríguez-Blas, T. *Dalton Trans.* **2006**, 5404−5415. (b) Ferreiros-Martinez, R.; Esteban-Gomez, D.; Platas-Iglesias, C.; de Blas, A.; Rodriguez-Blas, T. *Inorg. Chem.* **2009**, *48*, 10976−10987.
(44) Chatterton, N.; Gateau, C.; Mazzanti, M.; Pécaut, J.; Borel, A.; Helm, L.; Merbach, A. E. *Dalton Trans.* **2005**, 1129−1135.
(45) Amorim, M. T. S.; Delgado, R.; Fraústo da Silva, J. J. R. *Polyhedron* **1992**, *11*, 1891−1899.
(46) Chaves, S.; Delgado, R.; Fraústo da Silva, J. J. R. *Talanta* **1992**, *39*, 249−254.
(47) Burai, L.; Fabian, I.; Kiraly, R.; Szilagyi, E.; Brucher, E. *J. Chem. Soc., Dalton Trans.* **1998**, 243−248.
(48) Huskens, J.; Torres, D. A.; Kovacs, Z.; Andre, J. P.; Geraldes, C. F. G. C.; Sherry, A. D. *Inorg. Chem.* **1997**, *36*, 1495−1503.
(49) Weeks, J. M.; Taylor, M. R.; Wainwright, K. P. *J. Chem. Soc., Dalton Trans.* **1997**, 317−322.
(50) Williams, N. J.; Dean, N. E.; VanDerveer, D. G.; Luckay, R. C.; Hancock, R. D. *Inorg. Chem.* **2009**, *48*, 7853−7863.
(51) Reith, L. M.; Himmelsbach, M.; Schoefberger, W.; Knör, G. *J. Photochem. Photobiol., A* **2011**, *248*, 247−253.
(52) *Crysalis software system*, version 1.171.28 cycle4 beta; Oxford Diffraction Ltd.: Abingdon, U.K., 2005.
(53) SHELX: Sheldrick, G. M. *Acta Crystallogr.* **2008**, *A64*, 112−122.
(54) Glasoe, P. K.; Long, F. A. *J. Phys. Chem.* **1960**, *64*, 188−189.
(55) Tao, J. M.; Perdew, J. P.; Staroverov, V. N.; Scuseria, G. E. *Phys. Rev. Lett.* **2003**, *91*, 146401.
(56) Frisch, M. J.; Trucks, G. W.; Schlegel, H. B.; Scuseria, G. E.; Robb, M. A.; Cheeseman, J. R.; Scalmani, G.; Barone, V.; Mennucci, B.; Petersson, G. A.; Nakatsuji, H.; Caricato, M.; Li, X.; Hratchian, H. P.; Izmaylov, A. F.; Bloino, J.; Zheng, G.; Sonnenberg, J. L.; Hada, M.; Ehara, M.; Toyota, K.; Fukuda, R.; Hasegawa, J.; Ishida, M.; Nakajima, T.; Honda, Y.; Kitao, O.; Nakai, H.; Vreven, T.; Montgomery, Jr., J. A.; Peralta, J. E.; Ogliaro, F.; Bearpark, M.; Heyd, J. J.; Brothers, E.; Kudin, K. N.; Staroverov, V. N.; Kobayashi, R.; Normand, J.; Raghavachari, K.; Rendell, A.; Burant, J. C.; Iyengar, S. S.; Tomasi, J.; Cossi, M.; Rega, N.; Millam, N. J.; Klene, M.; Knox, J. E.; Cross, J. B.; Bakken, V.; Adamo, C.; Jaramillo, J.; Gomperts, R.; Stratmann, R. E.; Yazyev, O.; Austin, A. J.; Cammi, R.; Pomelli, C.; Ochterski, J. W.; Martin, R. L.; Morokuma, K.; Zakrzewski, V. G.; Voth, G. A.; Salvador, P.; Dannenberg, J. J.; Dapprich, S.; Daniels, A. D.; Farkas, Ö.; Foresman, J. B.; Ortiz, J. V.; Cioslowski, J.; Fox, D. J. *Gaussian 09*, revision A.01; Gaussian, Inc.: Wallingford, CT, 2009.
(57) Metz, B.; Stoll, H.; Dolg, M. *J. Chem. Phys.* **2000**, *113*, 2563−2569.
(58) (a) Ramírez, J.-Z.; Vargas, R.; Garza, J.; Hay, B. P. *J. Chem. Theory Comput.* **2006**, *2*, 1510−1519. (b) Casely, I. J.; Ziller, J. W.; Fand, M.; Furche, F.; Evans, W. J. *J. Am. Chem. Soc.* **2011**, *133*, 5244−5247.
(59) Tomasi, J.; Mennucci, B.; Cammi, R. *Chem. Rev.* **2005**, *105*, 2999−3093.
(60) (a) Peng, C.; Ayala, P. Y.; Schlegel, H. B.; Frisch, M. J. *J. Comput. Chem.* **1996**, *17*, 49−56. (b) Peng, C.; Schlegel, H. B. *Isr. J. Chem.* **1994**, *33*, 449−454.
(61) Wolinski, K.; Hilton, J. F.; Pulay, P. *J. Am. Chem. Soc.* **1990**, *112*, 8251−8260.
(62) Rega, N.; Cossi, M.; Barone, V. J. *J. Chem. Phys.* **1996**, *105*, 11060−11067.
(63) Barfield, M.; Fagerness, P. *J. Am. Chem. Soc.* **1997**, *119*, 8699−8711.
(64) Roger, M.; Lima, L. M. P.; Frindel, M.; Platas-Iglesias, C.; Gestin, J.-F.; Delgado, R.; Patinec, V.; Tripier, R. *Inorg. Chem.* **2013**, *52*, 5246−5259.
(65) Gran, G. *Analyst* **1952**, 661−671.
(66) Schwarzenbach, G.; Flaschka, W. *Complexometric Titrations*; Methuen & Co: London, 1969.
(67) Sweeton, F. H.; Mesmer, R. E.; Baes, C. F., Jr. *J. Solution Chem.* **1974**, *3*, 191−214.
(68) Gans, P.; Sabatini, A.; Vacca, A. *Talanta* **1996**, *43*, 1739−1753.
(69) Alderighi, L.; Gans, P.; Ienco, A.; Peters, D.; Sabatini, A.; Vacca, A. *Coord. Chem. Rev.* **1999**, *184*, 311−318.
(70) Gans, P.; Sabatini, A.; Vacca, A. *Ann. Chim.* **1999**, *89*, 45−49.

DOI: 10.1021/acs.inorgchem.5b01079
Inorg. Chem. 2015, 54, 7045−7057